24th ABCM International Congress of Mechanical Engineering
December 3-8, 2017, Curitiba, PR, Brazil

# COBEM-2017-5394
# EVALUATION OF ADHESIVES USED ON E/M IMPEDANCE METHOD APPLIED IN SHAFT UNDER FATIGUE TESTS

**Karina Mayumi Tsuruta**[1]
**Caroline Graciano Guimarães**[2]
**Diogo de Souza Rabelo**[3]
**Roberto Mendes Finzi Neto**[4]
**Aldemir Ap. Cavalini Jr.**[5]
**Valder Steffen Jr.**[6]
[1, 2, 4 ,5, 6] Federal University of Uberlândia, School of Mechanical Engineering, Av. João Naves de Ávila, 2121, Uberlândia, MG, 38408-196, Brazil.
[3] Federal Institute of Education, Science and Technology of Mato Grosso, Campus Primavera do Leste, Av. Dom Aquino, 1500, Primavera do Leste, MT, 78850-000, Brazil
[1]karinamt@ufu.br, [2]carolineguimaraes@ele.ufu.br, [3] diogo.rabelo@snp.ifmt.edu.br , [4]finzi@ufu.br, [5]aacjunior@ufu.br, [6]vsteffen@ufu.br

***Abstract.*** *The impedance-based structural health monitoring technique (SHM) has been widely investigated in the last years. This nondestructive method requires low-weight PZT patches with high frequency actuation/response capability to detect incipient damage in mechanical structures. However, the adhesive used to bond the transducers to the host structure can affect the performance of the technique. In this context, this paper is dedicated to evaluates the performance of PZT transducers bonded on steel shafts specimens by using three different adhesives, namely: epoxy 01, epoxy 02, and an ethyl-polyoxysilane based adhesive. Four PZT patches were bonded to each shaft. To evaluate the performance of the adhesives considering the shafts excited by dynamic loads, successive fatigue tests with 500,000 cycles were performed in each shaft. The stress applied to the shafts kept the specimens in the elastic phase. The acquisition of the impedance signatures was done considering two structural conditions, namely: i) pristine condition and ii) after each fatigue cycle. After ten successive fatigue tests, it was possible to observe that the adhesives used clearly presented different performances. It is worth mentioning that there are few studies regarding the effects of adhesive on the performance of the impedance-based SHM technique.*

***Keywords:*** *Adhesive, Electromechanical Impedance Method, Steel Shaft, SHM, Piezoelectric Transducers.*

## 1. INTRODUCTION

Humanity is directly dependent on mechanical structures and systems (aircraft, bridges, oil rigs, power and generation systems, rotating machines, etc.). However, some of these systems are at the end of the life which they were designed. And since their replacement is financially infeasible and maintenance shutdowns are costly, real-time damage detection devices have been developed in recent years with the objective to evaluate structural integrity of the systems (Farrar and Wonden, 2012)

In rotating systems, the methods of structural monitoring are commonly based on vibration signals and other sensors (temperature, pressure, speed, among others), without incorporating modern and robust techniques of damage identification (characterization). Therefore, specialists in this area have been developed structural health monitoring techniques (SHM techniques) capable to be applied in the machine during operation. Consequently, the costs involved are reduced and safety is increased.

The structural health monitoring based on the electromechanical impedance approach has been applied in rotor systems (Liang, Sun and Rogers, 1994). This method uses piezoelectric transducers coupled to the structure to monitor incipient damages. In this method, the electrical impedance of the PZT coupled to the mechanical system is measured. Assuming that the properties of PZT do not vary over time, changes in electrical impedance will be related to changes in mechanical impedance, which in turn is affected by the presence of damages. As the visual comparison is not enough, it is necessary to use quantitative criteria, in this case, damage metrics, which are scalar parameters capable of numerically representing the difference between two measurements.

However, the electromechanical impedance method presents some disadvantages, such as the false positive alarms obtained by the influence of the temperature and the fragility of the PZT patch (Rabelo et al., 2015). Some techniques were developed to evaluates the integrity of the piezoelectric transducers by using a self-diagnosis procedure, as presented by Park et al. (1996), Overly et al. (2007), and Grisso and Inman (2009). Rabelo et al. (2016) proposed an optimization approach able to compensate the influence of the temperature in the impedance signatures.

Various contributions in literature are dedicated to the analysis of the adhesive layer used the bond the PZT patch to the host structure. Qing et al. (2005) showed that the thickness of the adhesive layer alters the electromechanical impedance and the resonance frequency of the piezoelectric elements. Boehme, Roellig, and Wolter (2010) evaluated the influence of the viscoelastic properties of adhesives, proving that natural factors, such as humidity, can alter the results obtained by the SHM technique. Therefore, it is possible to conclude that the efficiency of the monitoring system is directly related to the characteristics of the adhesive used to bond the piezoelectric element to the host structure (thickness, stiffness, and eventual delamination of the adhesive layer) (Santana, 2007). In addition, degradation of the transducers may lead to a reduction in the ability to detect damage or to present false diagnoses (Wandowski, 2015). Therefore, the objective of this work is to evaluate the adhesive performance used to attached the PZT transducer in steel shafts of rotating machines under dynamic loads. In this case, three types of adhesives have been employed.

## 2. ELECTROMECHANICAL IMPEDANCE METHOD – A REVIEW

The ISHM technique become popular after the structure to monitor changes on its stiffness, damping, and mass. Due to the difficulty of obtaining the mechanical impedance of the structure, the electrical impedance measurements are acquired from piezoelectric transducers coupled to the host structure. Considering that the properties of the PZT patch (Lead Zirconate Titanate) do not vary over time, changes in the electrical impedance will be directly related to changes in the mechanical impedance, which is affected by the presence of damage (Liang, Sun and Rogers, 1994; Farrar, Lieven and Bemend, 2005; Park, Cudney and Inman, 2000; Park and Inman, 2005). A single-degree-of-freedom (DOF) electromechanical model that describes the measurement process is shown in Figure 1.

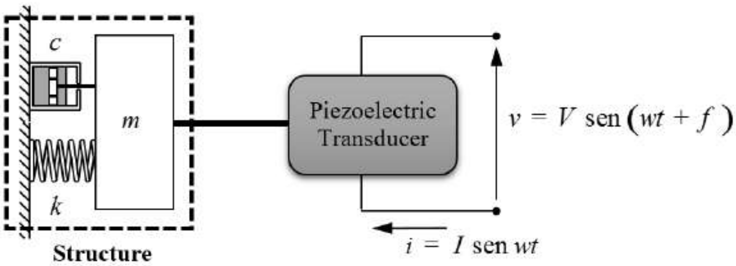


Figure 1 – A single DOF Electromechanical Model of the impedance-based structural health monitoring method (Liang, Sun and Rogers, 1994).

Based on the system shown in Fig. 1, the admittance $Y_a(\omega)$ of the piezoelectric transducer is a combined function involving the mechanical impedance of the PZT actuator $Z_{ma}(\omega)$ and the structure $Z_{me}(\omega)$, according to Eq. (1):

$$Y_a(\omega) = I(\omega)\omega a\left\{\varepsilon_{33}^T\left[1 - I(\omega)\delta\right] - \frac{Z_{ma}(\omega)}{Z_{ma}(\omega) - Z_{me}(\omega)} d_{3x}^2 \hat{Y}_{xx}^E\right\} \tag{1}$$

where $\hat{Y}^E_{xx}$ is the complex Young's modulus of the PZT patch with zero electric field, $d_{3x}$ is the piezoelectric coupling constant in the arbitrary $x$ direction at zero electric field, $\varepsilon^T_{33}$ is the dielectric constant at zero stress, $\delta$ is the dielectric loss tangent to the PZT patch, $a$ is a geometric constant of the PZT patch, and is $\omega$ the frequency. The impedance is a frequency dependent complex function. To obtain the electrical impedance, both the direct and inverse effects of the piezoelectric transducer are taken into account. The direct effect (or sensor effect) is characterized by producing a voltage when the piezoelectric transducer is mechanically deformed in the elastic phase, and the inverse effect (or actuator effect) appears when a piezoelectric ceramic patch is subjected to a voltage, resulting a mechanical deformation (Liang, Sun and Rogers, 1994; Farrar, Lieven and Bemend, 2005; Park, Cudney and Inman, 2000; Park and Inman, 2005).

### 2.1 Damage Metric

The detection and evaluation of the structure integrity is based on the comparison between the impedance signatures acquired from both the healthy and damaged (or unknown condition) structure. A visual examination of the signals is not enough for evaluation, since it gives only a qualitative comparison. Consequently, it is necessary to use an adequate metrics for defining quantitative criteria. Thus, damage metrics (DM) are employed, i.e., scalar parameters are properly defined so that they can numerically represent the difference between the two signals (without and with damage) (Naidu and Soh, 2004).

For the Impedance electromechanical approach, several DMs are proposed to evaluate the integrity of the structure (Palomino et al., 2011). As an example, one of the most commonly used is the RMSD (Root Mean Square Deviation) and its definition is given by Eq. 2 (Grisso, 2004 and Pears, 2006).

$$RMSD = \left\{ \sum_{i=1}^{n} \frac{\left[ \mathrm{Re}\left(Z_{1i}\right) - \mathrm{Re}\left(Z_{2i}\right) \right]^2}{\mathrm{Re}\left(Z_{1i}\right)^2} \right\}^{1/2} \tag{2}$$

where $\mathrm{Re}(Z_{1i})$ is the real part of the impedance measure without damage (baseline) at the frequency $i$. $\mathrm{Re}(Z_{2i})$ is the real part of the impedance measurement at the frequency $i$ for a new structural configuration and $n$ is the total number of points used in the measurements.

## 3. TEMPERATURE COMPESATION THROUGH OPTIMIZATION PROCEDURE

Temperature variation effects are known to cause horizontal (frequency) and vertical (amplitude) shifts in impedance signatures. A review of temperature variation effects and compensation methods can be found in (Rabelo et al., 2016; Baptista at al., 2016). Figure 2 shows a flowchart to illustrate the proposed temperature compensation approach. The method starts by obtaining the impedance signatures of the healthy system evaluated (Impbaseline; temperature Tbaseline). The impedance signatures of the system for an unknown condition (Impunknown; temperature Tunknown ≠ Tbaseline) are also required, so that the optimizer is responsible for shifting both the frequency and amplitude values. The Impunknown signatures are compared with the Impbaseline ones by means of a given objective function, i.e., a damage metric, as presented by Eq. (2) (Impbaseline = Z1 and Impunknown = Z2). In Fig. 2, if the procedure converges to a minimum value of the objective function, the effects of temperature variation are compensated through frequency shifts and vertical shifts of the design variables. If this is not the case, the optimization procedure continues the search for new frequency and amplitude shifts. The optimization process continues iteratively until convergence is assured, which can lead to temperature compensation (if the objective function is close to zero) or, otherwise, represents a damage indication associated with temperature compensation.

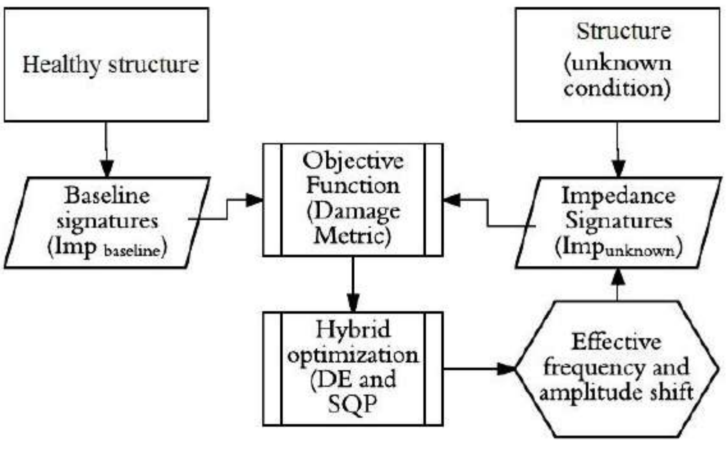


Figure 2 – Proposed temperature compensation flowchart.

In the present contribution, a hybrid optimization technique is primarily devoted to minimizing the influence of temperature variations during the impedance measurement process. The following section describes the proposed hybrid optimization algorithm. In this sense, the evolutionary technique known as Differential Evolution (DE) (Sun et al., 1995) is devoted to the global search for the optimum (i.e., the effective frequency and amplitude shifts). It is worth mentioning that the DE algorithm must be performed n times to avoid local minima. The best result obtained by DE is then used as a starting point for the classical direct method named Sequential Quadratic Programming (SQP) to obtain the local and refined optimal solution.

The DE algorithm is an optimization technique that belongs to the family of evolutionary computation, which differs from other evolutionary algorithms in the mutation and recombination schemes. DE executes its mutation operation by adding a weighted difference vector between two individuals to a third one. Then, the mutated individuals will perform discrete crossover and greedy selection with the corresponding individuals from the last generation to produce the offspring. The key control parameters of DE are the population size (NP), the crossover constant (CR), and the associated weight (F).

The pseudo-code of DE algorithm is presented in Fig. 3, in which P is the population of the current generation, and P' is the population to be constructed for the next generation, C[i] is the candidate solution with population index I, C[i][j] is the j-th entry in the solution vector of C[i], and r is a random number between 0 and 1. In (Pear, 2006), simple rules are given for choosing the key parameters of DE for general applications. Normally, NP should be about 5 to 10 times the dimension of the problem (i.e., the number of design variables). As for F, it lies in the range between 0.4 and 1.0. Initially, F = 0.5 can be tried, and then F and/or NP can be increased if the population converges prematurely. In (Price, Storm, and Pampinen, 2005) various mutation schemes where proposed for the generation of new candidate solutions by combining the vectors that are randomly chosen from the current population. In the applications presented in this paper, the rand / 1 scheme was used.

```
Differential Evolution
Initialize and evaluate population P
  while (not done) {
    for (i = 0; i < N; i++) {
      Create candidate C[i]
      Evaluate C[i]
       if (C[i] is better than P[i])
        P0[i] = C[i]
        else
        P0[i] = P[i]}
        P = P0
  }
Create candidate C[i]
Randomly select parents P[i1], P[i2], and P[i3]
where i, i1, i2, and i3 are different.
 Create initial candidate
  C'[i] = P[i1] + F×(P[i2]-P[i3]).
   Create final candidate C[i] by crossing over the genes of  P[i] and C'[i] as follows:
     for (j = 0; j < N; j++) {
      if (r <CR)
       C[i][j] = C'[i][j]
       else
      C[i][j] = P[i][j]
}
```

Figure 3 – Pseudo-code of DE algorithm.

The SQP algorithm is a direct method used for dealing with constrained minimization problems in which the search direction *S* is found by solving a sub problem with a quadratic objective function and linear constraints (Bendat and Piersol, 2000). For this purpose, a quadratic approximation of the augmented objective function (i.e., from the association of the Lagrange multipliers $\lambda$ with an exterior penalty technique) and a linear approximation for constraints are written, as shown in Eq. (3).

$$\begin{aligned} &\text{Minimize:} \quad Q(S) = F(X) + \nabla F(X)^T S + \frac{1}{2} S^T B S \\ &\text{Subject to:} \quad \nabla g_j(X)^T S + \delta_j g_j(X) \leq 0 \qquad j = 1, m \\ &\qquad\qquad\quad \nabla h_k(X)^T S + \bar{\delta} h_k(X) \leq 0 \qquad k = 1, l \end{aligned} \tag{3}$$

where *X* is the vector of design variables and *B* is initially an identity matrix that will be updated on subsequent iterations. The parameters $\delta_j$ and $\bar{\delta}$ are used to prevent inconsistences between the linearized constrains $g_j$ and $h_k$ (i.e., typically $0.9 \leq \bar{\delta} \leq 0.95$). The $\delta_j$ parameter is defined as follows:

$$\delta_j = 1 \quad if \;\; g_j(X) < 0$$
$$\delta_j = \bar{\delta} \quad if \;\; g_j(X) \geq 0 \tag{4}$$

The direction-finding problem described by Eq. (3) is actually a quadratic programming problem and special techniques should be used for its solution. The associated one-dimensional search is written from the determined search direction $S$ and an exterior penalty function $\phi$, as given by Eq. (5).

$$\phi = F(X) + \sum_{j=1}^{m} u_j \{\max[0, g_j(X)]\} + \sum_{k=1}^{l} u_{m+k} \left| h_k(X) \right| \tag{5}$$

where $X = X^{q-1} + \alpha_p S$, $u_j = |\lambda_j|$ ($j$ = 1, $m + l$) in the first iteration, $u_j$ = max [$|\lambda_j|$, 0.5 ($u'_j + |\lambda_j|$)] for the subsequent iterations, and $u'_j = u_j$ from the previous iteration. In this case, $\alpha_p = 1$.

## 4. EXPERIMENTAL PROCEDURE

In the experimental tests of the present paper, three steel specimens were made with the dimension showed in Fig. 4. In this case, two chamfers of 10 x 1 mm were made at the edges of the shaft for positioning purposes on the used MTS® test machine. Four PZT transduces were attached on the middle of the shaft, two PZT patches were bonded aligned with the chamfers and the other two patches were bonded at 90° in from the first two. Three types of adhesive were evaluated, namely: epoxy 01, epoxy 02, and an ethyl-polyoxysilane based glue. The same bonding process was used for all shaft specimens and adhesives.

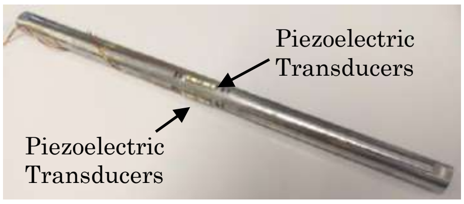


(a)

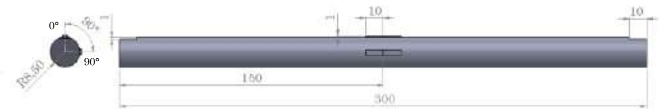


(b)

Figure 4 – (a) Shaft specimen with piezoelectric transducers; (b) Main dimensions.

To evaluate the behavior of each adhesive considering dynamic loads, the shaft specimens were positioned in the MTS® test machine as shows Fig. 5a. Figure 5b presents the scheme of the support and load rollers used to apply the loads on the shaft. Note that the specimens were submitted to a three-point fatigue test. During the tests, the PZT transduces attached in the bottom of the shaft (indicated by the letter *A* in Fig. 5b) were subject, predominantly, to normal stresses. The remaining sensors (indicated by the letter *A* in Fig. 5b) were subjected, predominantly, to shear stresses.

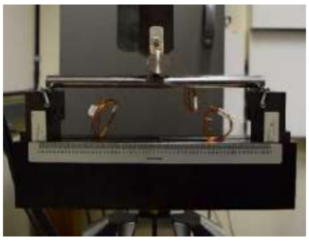

(a)

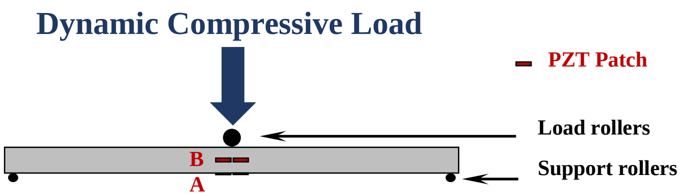


(b)

Figure 5 – (a) Specimen placed on an MTS® test machine; (b) Support and load applied on the shaft (three-point fatigue test).

For each run of the e MTS® test system, the shaft specimens were subjected to 500,000 cycles. The fatigue tests were carried out for a maximum displacement of 0.020 mm applied on the midspan of the shaft (see Fig. 5). This procedure was repeated ten times, as shows Tab. 1.

Table 1 – Test set-up.

| Run | Test | Indication |
|---|---|---|
| Baseline | Baseline | **B** |
| 1 | 500,000 cycles | **1** |
| 2 | 500,000 cycles | **2** |
| 3 | 500,000 cycles | **3** |
| 4 | 500,000 cycles | **4** |
| 5 | 500,000 cycles | **5** |
| 6 | 500,000 cycles | **6** |
| 7 | 500,000 cycles | **7** |
| 8 | 500,000 cycles | **8** |
| 9 | 500,000 cycles | **9** |
| 10 | 500,000 cycles | **10** |

A portable impedance meter device was used to measure the impedance signatures (see Fig. 6b). In this case, 5000 points in a frequency range from 30 kHz to 50 kHz were considered. For each test presented in Tab. 1, 30 measurements were obtained. All data acquisition was done inside the environmental test chamber configured to maintain 25°C (see Fig. 6a). Additionally, in each measurement made by the impedance device, the temperature was measured.

(a)


(b)

Figure 6 – (a) Environmental test chamber; (b) portable impedance meter device (SySHM impedance meter).

## 5. RESULTS AND DISCUSSION

Figures 7 and 8 show the results obtained from the PZT transducers attached in the shaft specimens by using the epoxy 1. Figures 7a, 7b, and 8a present the measured impedance signatures without temperature compensation, with temperature compensation, and the mean value of the compensated impedance signatures associated with each test presented in Tab. 1, respectively. It is worth mentioning that the vertical shifts observed in the impedance measurements of Fig. 7a are caused by temperature variation in the thermal chamber (Mean value: 24,98 °C; STDEV: 1,45 °C).

Figure 8b shows the values of the damage metric obtained before and after the application of the compensation procedure in the impedance signatures measured from the PZT#1 and by using the epoxy 1. Regarding the values of the damage metrics associated with the compensated impedance signatures, a slight variation is observed only on the results by comparing the baseline and first step of tests. Thus, the epoxy 1 presents a satisfactory performance when the host structure is exposed to the dynamic loads.

Figure 9 shows the results obtained from the PZT#5 attached on the shaft specimens by using the epoxy 2. Figure 9a shows the mean value of the compensated impedance signatures (similar to Fig. 8a). Figure 9b shows the values of the damage metric obtained before and after the application of the compensation procedure in the impedance signatures (similar to Fig. 8b). Regarding the values of the damage metrics associated with the compensated impedance signatures, it can be observed that the obtained values increase according to the applied fatigue tests. Similar results can be observed by using the PZT#9 attached to the shaft specimens by using the ethyl – Polyoxysilane based glue (see Fig. 10). Therefore, epoxy 2 and ethyl – Polyoxysilane based glue presents a non-satisfactory performance when the host structure is exposed to the dynamic loads.

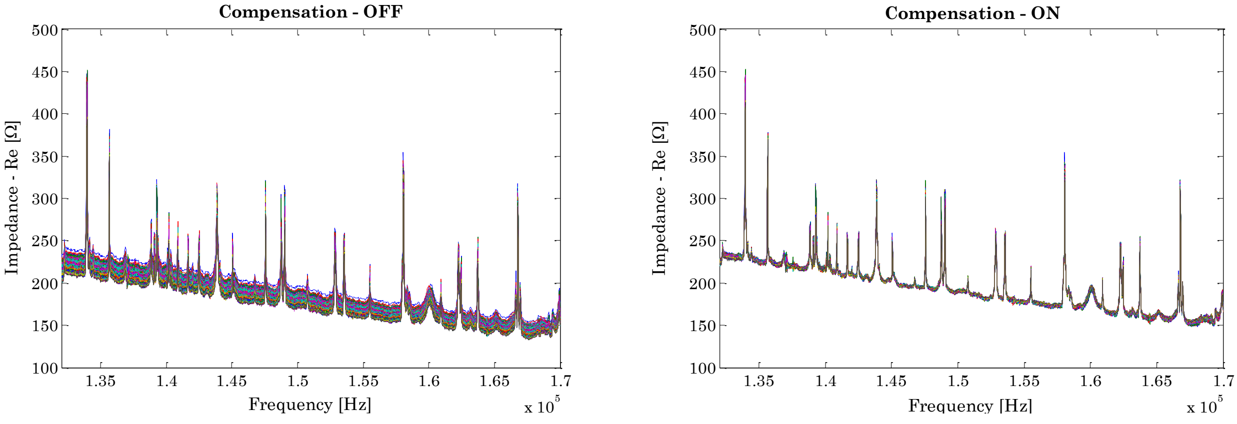


(a) (b)

Figure 7 – Epoxy 1 - Impedance signatures: (a) Compensation OFF; (b) Compensation ON.

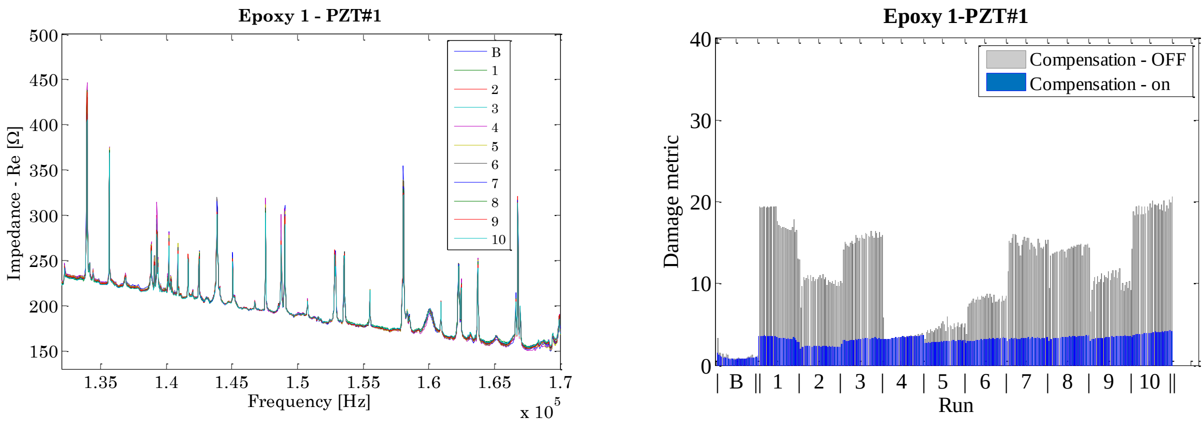


hui(a) (b)

Figure 8 – Epoxy 1 (PZT#1) – (a) Impedance signatures (compensation ON); (b) Damage metric (0°).

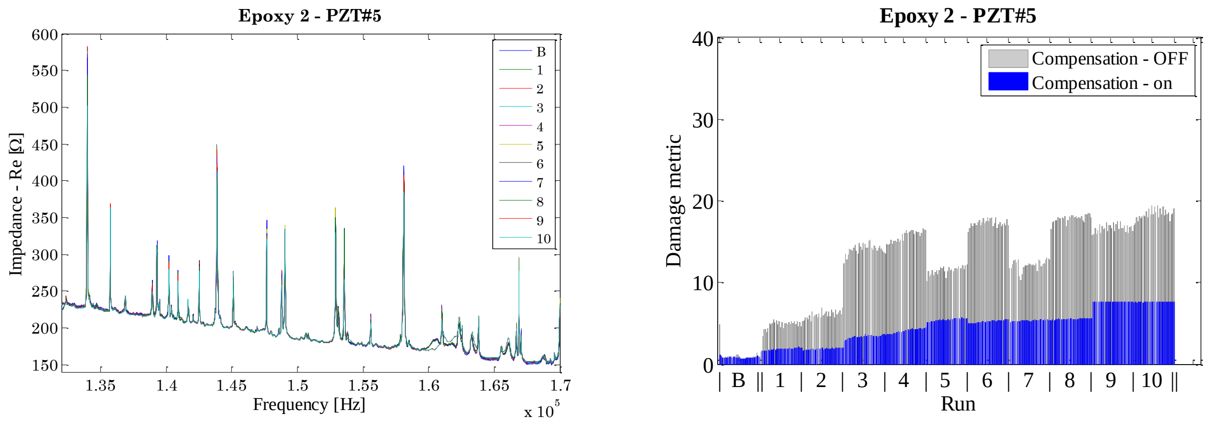


(a) (b)

Figure 9 – Epoxy 2 (PZT#5) – (a) Impedance signatures (compensation ON); (b) Damage metric (0°).

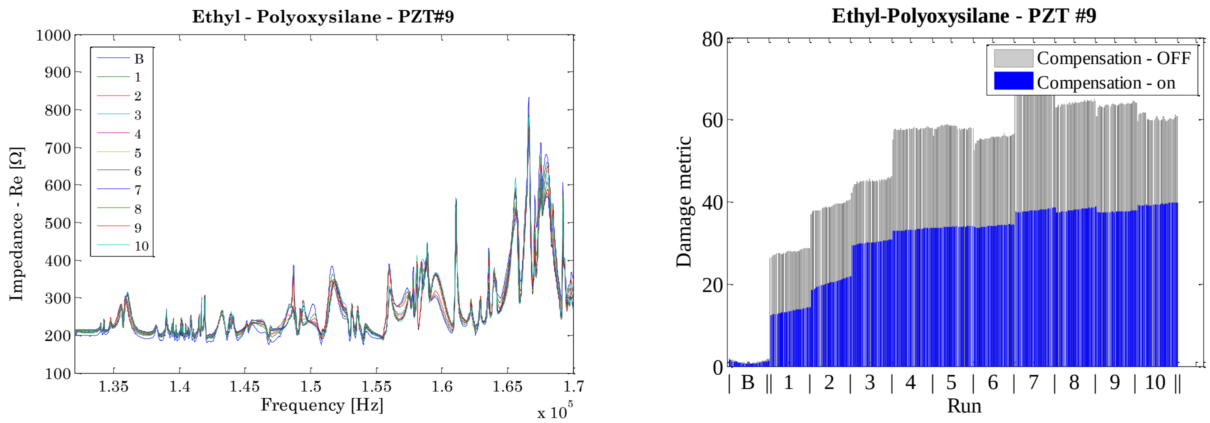


(a) (b)

Figure 10 – Ethyl - Polyoxysilane (PZT#9): (a) Impedance signatures (compensation ON); (b) Damage metric (0°).

## 6. CONCLUSIONS

In this paper, the performance of PZT transducers bonded on shafts with different types of adhesive was evaluated. For this aim, piezoelectric sensors were bonded to steel shaft specimens by using three different adhesives, namely: epoxy 01, epoxy 02, and an ethyl-polyoxysilane based glue. Four PZT patches were bonded to each shaft. To evaluate each adhesive, successive fatigue tests with 500,000 cycles each were performed in the shafts. Based on the results, the adhesive used to bond the piezoelectric transducers under fatigue tests can interfere in the results obtained by using the structural health monitoring technique based on electromechanical impedance approach. Comparing the performance of the considered adhesives, the epoxy 1 demonstrated to be better adapted to dynamic loads, since the value of damage metric remained almost constant after the first run of the fatigue tests. Further research effort will be dedicated to evaluating the performance of the same adhesives applying the conveyed methodology in a rotating machine.

## 7. ACKNOWLEDGEMENTS

The authors are thankful to the Brazilian Research Agencies CAPES, CNPq (574001/2008-5 and 152334/2016-5) and FAPEMIG (TEC-APQ-022284-15 / TEC-APQ-307609) for the financial support provided to this research effort.

## 8. REFERENCES

Baptista, F.G, Budoya, D.E, Almeida, V.A.D., Ulson, J.A.C., An experimental study on the effect of temperature on piezoelectric sensors for impedance-based structural health monitoring. Sensors 14(1): 1208-1227. 2014. doi: 10.3390/s140101208

Bendat, J. S, Piersol, A. G., Random data – analysis and measurement procedures, John Wiley and Sons. New York, 2000.

Boehme, B.; Roellig, M.; Wolter, K.-J. Measurements of Viscoelastic Material Properties of Adhesives for SHM Sensors under Harsh Environmental Conditions. In: 11th. Int. Conf. on Thermal, Mechanical and Multiphysics Simulation and Experiments in Micro-Electronics and Micro-Systems. EuroSimE. 2010.

Farrar, C. R and Wonden, K. Structural Health Monitoring: A Machine Learning Perspective, Willey and sons Ltda, 2012.

Farrar, C. R., Lieven, N. A. J., Bemend, M. T., "An introduction to damage prognosis". Inman, C. R. Farrar, V. Lopes Jr, V. Steffen Jr (Eds). John Wiley & Sons, ISBN: 978-0-470-86907-9, 2005.

Giurgiutiu, V., Zagrai, A., Damage detection in thin plates and aerospace structure with the electro-mechanical impedance method. Structural Health Monitoring. V.42, 99-118, 2005.

Grisso, B. L., Considerations of the impedance method, wave propagatiom. Amd wireless systems for structural health monitoring, 2004. 108f. Dissertation, Virginia Polytechnic Institute and State University, Virginia.

Grisso, B. L.; Inman, D. J. Temperature corrected sensor diagnostics for impedance-based SHM. Journal of Sound and Vibration. V. 329. p. 2323-2336. 2009.

Liang, C., Sun, F. P., Rogers, C. A, Coupled Electromechanical Analysis of Adaptive Material Systems – Determination of the Actuator Power Consumption and System Energy Transfer", Journal of Intelligent Material Systems and Structures, Vol. 5, pp. 12–20, 1994.

Liang, C., Sun, F. P., Rogers. C. A., Coupled Electro-Mechanical Analysis of Adaptive Material Systems-Determination of the Actuator Power Consumption and System Energy Transfer. Journal Intelligent Material Systems and Strutctures, 5, pp. 12-20, 1994.

Naidu, A. S. K, Soh C. K., Damage severity and propagation characterization with admittance signatures of piezo transducers. Journal Smart Materials and Structures, 13, 393-403, 2004.

Overly, T. G. S., Park. G., Farrar, C. R. Development of Signal Processing Tools and Hardware for Piezoelectric Sensor Diagnostic Processes. Proceedings of 14th SPIE Conference on Smart Structures and Nondestructive Evaluation, San Diego, USA, 2007.

Palomino, L. V., Moura Jr., J. R.V., Tsuruta, K. M., Rade, D.A., Seffen Jr., V., Impedance-based health monitoring and mechanical testing of structures. Smart Structures and Systems, V. 7, No.1, pp. 15-25, 2011.

Park, G., Cudney, H., Inman, D. J, Impedance-based health monitoring of civil structural components. ASCE Journal of Infrastructure Systems, 6, 153-160. 2000.

Park, G., Inman, D. J., Damage, D. J., Prognosis for Aerospace, Civil and Mechanical System. Chapter 13 "Impedance-Based Structural Health Monitoring". Inman, C. R. Farrar, V. Lopes Jr, V. Steffen Jr (Eds). John Wiley & Sons, ISBN: 978-0-470-86907-9, 2005.

Park, G.; Farrar, C. R.; Rutherford, A. C.; Robertson, A. N. Piezoelectric Active Sensor Self-Diagnostics using Electrical Admittance Measurements, ASME Journal of Vibration and Acoustics. V. 128(4). p. 469-476, 2006.

Peairs, D. M., High Frequency Modeling and Experimental Analysis for Implementation of Impedance-based Structural Health Monitoring. 2006. 150 f. Thesis – Virginia Polytechnic Institute and State University, Virginia.

Price, K.V., Storn, R.M., Lampinen, J.A., (2005) Differential evolution – a practical approach to global optimization. Springer. Heidelberg, Germany.

Qing, X. P.; Chan, H.-L.; Beard, S. J.; Ooi, T. K.; Marotta, S. A. Effect of adhesive on the performance of piezoelectric elements used to monitor structural health. International Journal of Adhesion & Adhesives. V. 26. p. 622-628, 2005.

Rabelo D. S., Steffen Jr. V., Finzi Neto R. M., Lacerda H.B., Impedance-based structural health monitoring and statistical method for threshold-level determination applied to 2024-T3 aluminum panels under varying temperature. Structural Health Monitoring 1(1): 1-17, 2016.

Rabelo, D. S.; Steffen Jr. V.;. Finzi Neto, R. M; Lacerda, H. B., A statistical approach for assessing reliability for impedance-based structural health monitoring using probability of detection. In: Proceedings of the 10th international workshop on structural health monitoring, 01-03 September 2015, pp. 707-714. Palo Alto, CA, USA: DES-tech Publications.

Santana, D.C. Modeling and optimization of shunts apply to passive vibration control. 2007. 203 f. Thesis, Federal University of Uberlândia Uberlândia.

Sun FP, Chaudhry Z, Liang C, Rogers CA (1995) Truss structure integrity identification using PZT sensor-actuator. J. Intell. Mater. Syst. Struct. 6(1): 134-139. doi: 10.1177/1045389X9500600117

Wandowski, T.; Moll, J.; Malinowski, P.; Opoka, S.; Ostachowicz, W. Assessment of piezoelectric sensor adhesive bonding. In: 11th International Conference on Damage Assessment. DAMAS, 2015.

## 9. RESPONSIBILITY NOTICE

The author(s) is (are) the only responsible for the printed material included in this paper.